

## Glass Dynamics and Domain Size in a Solvent-Polymer Weak Gel Measured by Multidimensional Magnetic Resonance Relaxometry and Diffusometry

Nathan H. Williamson,<sup>1</sup> April M. Dower,<sup>1</sup> Sarah L. Codd,<sup>2</sup> Amber L. Broadbent,<sup>3</sup> Dieter Gross,<sup>4</sup> and Joseph D. Seymour<sup>1,\*</sup>

<sup>1</sup>*Department of Chemical and Biological Engineering Montana State University, Bozeman, Montana 59717-3920, USA*

<sup>2</sup>*Department of Mechanical and Industrial Engineering, Montana State University, Bozeman, Montana 59717, USA*

<sup>3</sup>*Bend Research Incorporated, Lonza, Bend, Oregon 97701, USA*

<sup>4</sup>*Bruker Biospin Corp., 76275 Ettlingen, Germany*



(Received 27 March 2018; revised manuscript received 7 November 2018; published 12 February 2019)

Nuclear magnetic resonance measurements of rotational and translational molecular dynamics are applied to characterize the nanoscale dynamic heterogeneity of a physically cross-linked solvent-polymer system above and below the glass transition temperature. Measured rotational dynamics identify domains associated with regions of solidlike and liquidlike dynamics. Translational dynamics provide quantitative length and timescales of nanoscale heterogeneity due to polymer network cross-link density. Mean squared displacement measurements of the solvent provide microrheological characterization of the system and indicate glasslike caging dynamics both above and below the glass transition temperature.

DOI: 10.1103/PhysRevLett.122.068001

The drying of solvent-polymer solutions is important in industrial, biomedical, and environmental systems. Relevant systems range from drying paints or dyes [1] to spray drying materials in food and pharmaceutical processing [2,3], and from energy materials [4] to biomedical systems in wound healing and drug delivery [5]. Drying processes are mediated by formation of a film of polymer through which solvent transport from solution to gas phase occurs [1]. The reversible change in phase of the polymer-solvent system from liquid solution to amorphous solid phase during drying has been treated as a glass transition [6,7] and a gelation process [1,8], depending on concentration and temperature of the system. In solvent evaporative drying, chemical cross-links are not typically formed, rather gel formation is due to an entanglement network or physical gel, referred to as a weak gel [9–11]. The relationship between gelation and glass transitions is a topic of intense current theoretical interest with a multitude of simulations for reversible polymer gels [7,12–14], but experimental studies focused primarily on colloidal systems [15]. An outstanding question regarding these amorphous solids is, what is a concentrated macromolecular solution above and near its glass transition temperature: a weak gel, a glass, or a solution? [11,16]. Here, nuclear magnetic resonance (NMR) measurements of rotational and translational molecular dynamics of solvent molecules in a solvent-polymer system are used to characterize system dynamic heterogeneity [14]. The solvent molecular dynamics exhibit translational diffusion with glasslike caging behavior above the glass transition temperature indicating a molecular dynamics landscape, that has solid- and liquidlike regions of free volume in the physical weak gel phase [7,11,12,14,17]. The solvent dynamics allow determination

of a mesoscopic length scale associated with the physical cross-link density variations of the polymer [9] network [18], or liquid-solid free volume domain separation of a thermodynamic glass model [17]. The thermodynamic model indicates a second order type transition with associated divergence of isothermal compressibility and heat capacity [17,19,20]. It posits spatial domains of free volume in which molecular motion is either liquidlike  $v > v_c$  or solidlike  $v < v_c$ , above or below a critical free volume  $v_c$  determined by the form of the intermolecular free energy to break out of a cage of neighboring molecules [17]. The NMR methods applied are well established for the characterization of porous media structure [21–24], but represent a novel approach to the characterization of phase transition dynamics in polymer-solvent systems, using the solvent dynamics as a microrheology probe [25,26].

Simulations of reversible gelation for an attractive potential energy  $\epsilon$  of “sticky” monomers greater than the thermal energy  $\epsilon/k_B T > 1$ , display a plateau region in the polymer molecules mean squared displacement (MSD)  $\langle z^2(t) \rangle$  [7,12,14]. This plateau in the MSD is a well-established feature of dynamics in glass forming systems of molecules and colloids due to the caging effect [27,28]. Molecules in hard sphere model glass-forming liquids freely move on timescales shorter than the time to encounter another molecule show ballistic motion  $\langle z^2(t) \rangle \sim t^2$  within the cage of neighbors [27]. At longer displacement times diffusive dynamics  $\langle z^2(t) \rangle \sim t$  are observed after breaking out of the cage [27]. The origin of glasslike MSD dynamics of polymer molecules in reversible polymer gels is more complicated due to the interplay of thermodynamics, chemical kinetics, and polymer physics [12]. Classic characterization of gel network structure is based on a mesh

size, or correlation length  $\xi$  between cross-links that enters into scaling relations for material properties [8]. As solvent concentration or temperature decreases, a polymer network which spans the system has a solidlike elastic material response, and has been used as a definition of the gel phase transition [13]. A longer mesoscale length  $\Xi$  due to spatial variation of the microscale cross-link density related to network nanostructural heterogeneity develops with decrease in concentration or temperature [18]. Light scattering data on the length- and timescales of dynamics in polymer-solvent systems have indicated the existence of this slow, long length scale dynamics, but were treated skeptically until recently [29,30]. The NMR data presented provide direct measurement of a length scale that characterizes gel microstructure in terms of exchange of solvent molecules between regions of dynamic heterogeneity.

NMR has been applied to characterize domain sizes, structure, and nonergodic behavior in the glass transition [31–34] and gelation [35,36] behavior of polymers and molecular liquids. Pulsed gradient spin echo (PGSE) NMR measurement of translational diffusion has been broadly applied to polymer solutions, gels, and melts [37–40]. While some of these NMR applications measured solvent phase dynamics [31,36,41], the majority measure polymer dynamics. This work measures solvent dynamics using NMR porous media characterization methods [21–24,42,43] in which translational and rotational diffusion of the pore filling fluid probe pore microstructure. Analogously, the network nanostructure and heterogeneity of solvent-polymer systems is measured by the solvent dynamics in the data presented here.

The solvent-polymer system studied, hydroxypropyl methylcellulose acetate succinate MG (HPMCAS-MG) (Shin-Etsu Chemical Co.) in acetone, is broadly used in pharmaceutical spray drying applications and is of technological and theoretical interest [2,29]. The random substitution of acetyl, succinoyl, methoxyl, and hydroxypropoxy groups inhibits cellulose ordered structure which results in crystalline sheet structures, providing amorphous structure at high polymer concentration [2,44]. Data on HPMCAS/acetone samples over a range of concentrations (99% to 2%wt acetone), temperatures and aging times have been obtained and will be presented elsewhere [45]. The sample focused on in this Letter is 7% wt acetone (93% wt HPMCAS) [46]. It was prepared by five repetitions of evaporating acetone at ambient conditions and re-filling the 5 mm NMR tube with HPMCAS/acetone solution to obtain a polymer-rich sample of sufficient volume to occupy the active region of the NMR rf coil. Drying, from 11% wt acetone to 7% wt acetone, occurred over 270 days to ensure complete relaxation of any stresses induced in loading the sample. The glass transition temperature  $T_g$  of the HPMCAS/acetone mixture estimated from the Fox equation [47,48] is  $T_g = 19$  C at 11% wt acetone, and  $T_g = 47$  C at 7% wt acetone. During the 270 days storage

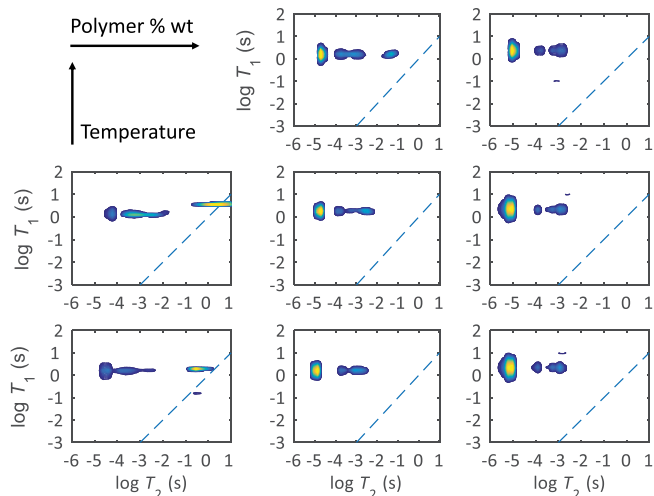


FIG. 1. Glass transitions indicated by  $T_1$ - $T_2$  distributions of 45% wt acetone (column 1), 7% wt acetone (column 2), and 2.3% wt acetone SDD (column 3) at 60 (top row), 22 (middle row), and  $-18$  °C (bottom row). The glass transition temperatures for these concentrations are  $-131$ ,  $47$ , and  $93$  °C, respectively. The dashed line is the parity line  $T_1 = T_2$  for liquidlike behavior.

at 22 °C, the sample dried from a rubbery state  $T_g < T_{\text{ambient}}$  to a glassy state  $T_g > T_{\text{ambient}}$ . A 45% wt acetone sample,  $T_g = -131$  °C and 2.3% wt acetone wet spray-dried dispersion (SDD),  $T_g = 93$  °C are also presented to elucidate the NMR relaxometry glass transition characterization [46].

NMR measurements were performed on a Bruker Avance III spectrometer at  $^1\text{H}$  resonance frequency of 250.12 MHz. A purpose built high-power rf probe with a 5 mm rf coil allowed short excitation pulses (3.5–7  $\mu\text{s}$ , 100 W). A Diff30 coil provided 17.82 T/m gradient strength in one axis. This hardware allowed novel measurements of magnetic relaxation times and translational diffusion at low solvent concentration [46].

$T_1$ - $T_2$  magnetic relaxation correlation experiments characterize the solid or liquid phase behavior of systems through the rotational and translational molecular diffusion dynamics [49]. Fast rotational diffusion of molecules averages out dipolar coupling resulting in longer spin-spin  $T_2$  relaxation times. Liquids are characterized by  $T_1 \approx T_2$  with values on the order of hundreds of ms to larger than 1 s. Solids have long  $T_1$  and short  $T_2$  relaxation times, with relative increases in  $T_1$  and decreases in  $T_2$  for more ordered crystalline phases [32,49]. Data in Fig. 1 demonstrate the ability of  $T_1$ - $T_2$  correlations to characterize the glass transition as a function of concentration and temperature variation. There are two distinct populations at short  $T_2$ : one of the order  $10^{-5}$  s from protons on the polymer backbone and another in the region  $10^{-4}$ – $10^{-3}$  s from polymer pendant group protons, indicating solidlike rotational mobility. These contain signal from protons on polymer and polymer associated solvation acetone. There is

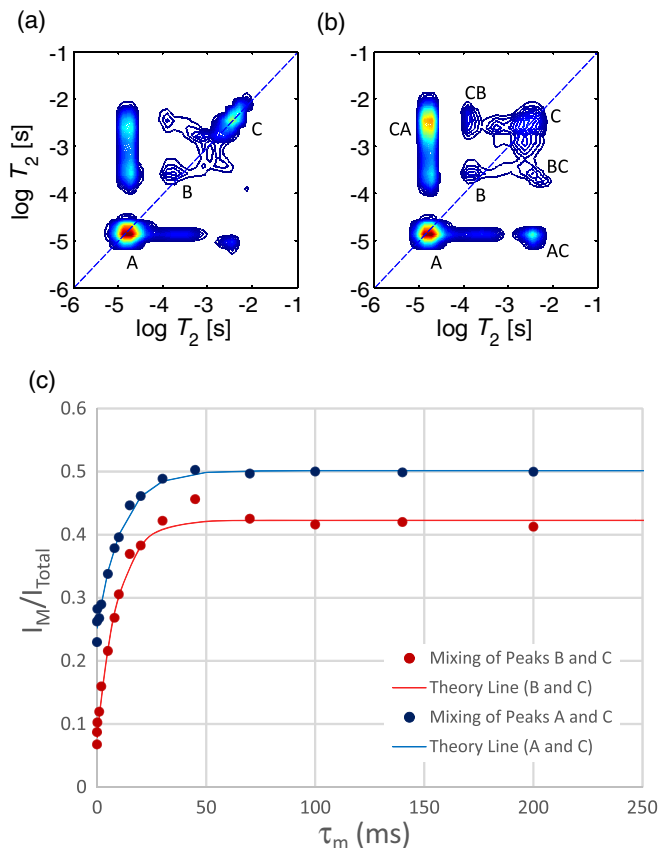


FIG. 2.  $T_2$ - $T_2$  exchange distributions of the 7% wt acetone/HPMCAS sample at 22°C for two of the mixing times (a)  $t_m = 1$  ms and (b)  $t_m = 100$  ms. (c) Calculated mixing peak intensities as a function of  $T_2$ - $T_2$  mixing time. Exchange model fit (red;gray) between populations  $B$  and  $C$  with exchange correlation time  $\tau_{\text{corr}} \sim 9.5$  ms (95% confidence interval [8.0, 10.9]). Exchange model fit (blue;black) between populations  $A$  and  $C$  with exchange correlation time  $\tau_{\text{corr}} \sim 11$  ms (95% C.I. [9.2,12.9]). Using the acetone diffusion coefficient  $D = 1.1 \times 10^{-12}$  m<sup>2</sup>/s measured for the sample at 22°C gives a correlation length between populations  $B$  and  $C$  of  $l_{\text{corr}} \sim 250$  nm and between populations  $A$  and  $C$  of  $l_{\text{corr}} \sim 270$  nm.

a third population that shifts from liquidlike ( $T_2 \sim 1$  s) to solidlike mobility with increasing concentration or decreasing temperature, merging with the other two populations, during the glass transition. This population is signal from protons on unassociated, nonsolvation complex solvent acetone, and the  $T_2$  shift visualizes dynamic arrest. The three populations directly indicate the system dynamic heterogeneity in terms of rotational diffusion.

$T_2$ - $T_2$  exchange experiments provide data on the translational diffusion mediated exchange between populations of differing rotational mobility [22,24,50].  $T_2$ - $T_2$  data for 7% wt acetone are shown for temperatures of 22°C (Fig. 2) and 60°C (Fig. 3), below and above  $T_g$ , respectively. Three primary populations of  $T_2$  along the diagonal are identified as described earlier. The two shortest  $T_2$  populations ( $A$  and  $B$ ) come from polymer and associated acetone and the

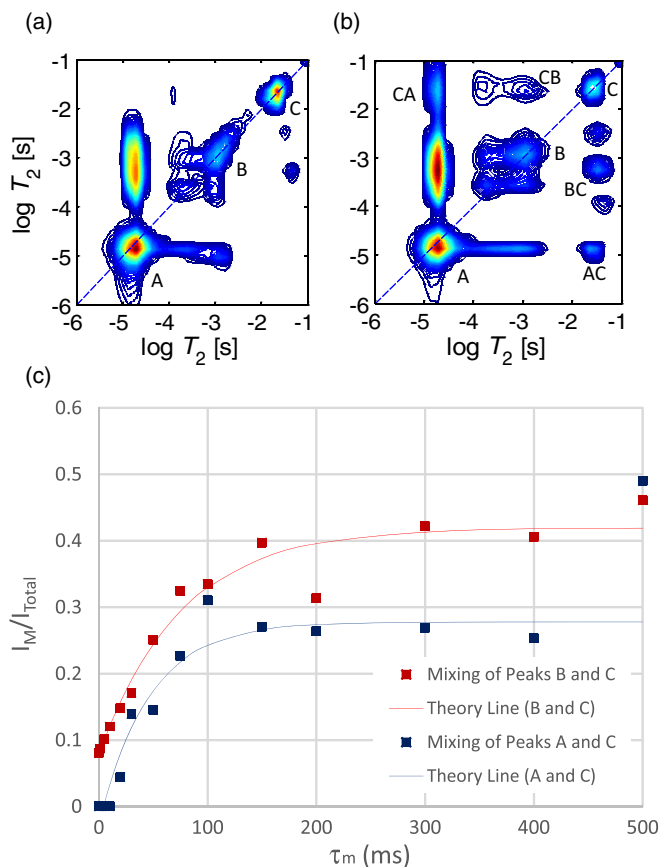


FIG. 3.  $T_2$ - $T_2$  exchange distributions of the 7% wt acetone/HPMCAS sample at 60°C for two of the mixing times (a)  $t_m = 1$  ms and (b)  $t_m = 100$  ms. (c) Calculated mixing peak intensities as a function of  $T_2$ - $T_2$  mixing time. Exchange model fit (red;gray) between populations  $B$  and  $C$  with exchange correlation time  $\tau_{\text{corr}} \sim 75$  ms (95% C.I. [44.1,105.9]). Exchange model fit (blue;black) between populations  $A$  and  $C$  with exchange correlation time  $\tau_{\text{corr}} \sim 46$  ms (95% C.I. [23.8,69.1]). Using the acetone diffusion coefficient  $D = 3.5 \times 10^{-12}$  m<sup>2</sup>/s measured for the sample at 60°C gives a correlation length between populations  $B$  and  $C$  of  $l_{\text{corr}} \sim 1.3$   $\mu\text{m}$  and between populations  $A$  and  $C$  of  $l_{\text{corr}} \sim 980$  nm.

longest  $T_2$  population ( $C$ ) from unassociated solvent acetone, as indicated above in the  $T_1$ - $T_2$  data. 2D distributions for mixing times of  $t_m = 1$  ms and 100 ms are shown for each temperature in Figs. 2(a), 2(b) and Figs. 3(a), 3(b). It is clear from Figs. 2 and 3 from the presence of off-diagonal cross peaks that significant exchange of spins between populations has occurred by 1 ms and that exchange increases with increased mixing time and higher temperature. The choice of acetone as solvent for these studies means chemical exchange of protons is not present so any exchange is due to diffusion of acetone between regions of different mobility [51]. Note the exchange peaks between populations  $A$  and  $B$  are nearly saturated in intensity by  $t_m = 1$  ms indicating rapid exchange between solvation acetone associated with the polymer backbone and pendant groups.

The current state of the art regarding exchange in  $T_2$ - $T_2$  NMR data is limited to two site exchange models and development and interpretation of three site exchange models is ongoing [52]. To extract quantitative information from the data, a modification of the two site exchange model of Washburn and Callaghan based on molecular conservation is applied [24]. The data indicate a nonzero initial condition, treated as  $t=0$  in the model  $N_{AB}(0) = N_{AB0}$ , accounting for exchange which has occurred at the shortest mixing time accessible, leading to  $N_{AB}(t) = [(N_B\tau_{AB}/\tau_{AB} + \tau_{BA}) - N_{AB0}][1 - \exp(-\lambda t)] + N_{AB0}$ . The number of exchanging spin bearing molecules  $N_{AB}(t)$  is given by the off-diagonal population intensities in the 2D data. The model, with three parameters  $[(N_B\tau_{AB})/(\tau_{AB} + \tau_{BA})]$ ,  $N_{AB0}$ , and  $\lambda$ , can be fit to the off-diagonal peak intensity data to determine the diffusive exchange correlation time  $\tau_{\text{corr}} = \lambda^{-1}$  through  $\lambda = \tau_{AB}^{-1} + \tau_{BA}^{-1}$ . Using this model, excellent fits to the data are found for the 22 °C data [Fig. 2(c)] below  $T_g$  and reasonable agreement at 60 °C above  $T_g$  [Fig. 3(c)], validating the independent two-site exchange approximation [24]. A correlation mixing time based length scale,  $l_{\text{corr}} = (6D_o\tau_{\text{corr}})^{1/2}$  can be determined if the data are in the fast diffusion limit, which for porous media is defined as the translational diffusion sampling of microstructure pore length scale  $a$ ,  $D_o/a^2$  being rapid compared to surface relaxation rates  $\rho/a$ , such that the ratio of surface relaxation rate to the diffusion rate  $k = \rho a/D_o \ll 1$  [46,53]. The length scale  $l_{\text{corr}}$  is a measure of the mesoscale length scale  $\Xi$ , the separation length of high cross-link density regions in terms of gel heterogeneity or the solidlike free volume regions of glass theory. Fitting the two-site model to exchange between the most mobile liquidlike population  $C$ , independently to each of the other populations results in  $\tau_{\text{corr}} \sim 9.5$  ms,  $l_{\text{corr}} = 250$  nm between populations  $B$  and  $C$  and  $\tau_{\text{corr}} \sim 11$  ms,  $l_{\text{corr}} = 270$  nm between populations  $A$  and  $C$  at 22 °C. In contrast at 60 °C  $\tau_{\text{corr}} \sim 75$  ms,  $l_{\text{corr}} = 1.3$   $\mu\text{m}$  between populations  $B$  and  $C$  and  $\tau_{\text{corr}} \sim 46$  ms,  $l_{\text{corr}} = 980$  nm between populations  $A$  and  $C$ . Statistical equivalence of the exchange correlation time and length for populations  $A$  and  $C$  and  $B$  and  $C$  at each temperature is due to rapid diffusive exchange amongst solvation acetone molecules in the solidlike domains of the backbone  $A$  and pendant group  $B$  populations, consistent with the two-site exchange approximation.  $T_1$ - $T_2$  correlation data are used to test for diffusive coupling, following the method of Song *et al.* [21,46]. At 22 °C, the fast diffusion limit is valid and the use of the diffusion to obtain a length scale  $l_{\text{corr}}$  is supported, while above  $T_g$  the solvent diffusion is coupled between the domains and the extracted length scale is more complicated to physically interpret [46].

Direct measurement of the displacement time-dependent translational diffusion of the acetone using PGSE NMR allows spectral resolution of the frequency domain chemical shift of the protons on the polymer and acetone

molecules. A limitation is the relatively long echo times of the order of  $\tau_{\text{PGSE}} \sim 1.5$  ms required to apply pulsed magnetic gradient fields and the accompanying loss of signal from the fast relaxing populations of spins with  $T_2 < \tau_{\text{PGSE}}$  [46]. PGSE NMR is well established to characterize porous media structure through the hindrances imposed on diffusing fluid molecules. The decrease in the diffusion coefficient is plotted as a function of increasing diffusion length scale or experimental displacement observation time  $\Delta$  [22,23]. A fit to the short time data provides the surface to volume ratio  $S/V_p$ , the pore length scale  $a \sim V_p/S$ , from  $D_{\text{eff}}(\Delta) = D_0[1 - (D_0\Delta)^{1/2}(S/V_p)]$  [23]. Fitting the acetone data to this model in Fig. 4(a) yields length scales of 590 nm at 22 °C and 1.2  $\mu\text{m}$  at 60 °C. Length scales obtained from this type of fit for the polymer system are not as reliable as for fluid filling a solid porous matrix, due to the inability to sample the diffusive displacement on timescales of the free diffusion, where the first order  $\Delta^{1/2}$  of the model is valid. This difficulty can be circumvented by applying the more informative micro-rheology approach plotting the MSD  $\langle z^2(\Delta) \rangle$  as a function of the displacement observation time  $\Delta$  as in Fig. 4(b) [25]. A plateau in MSD as observed in glasses and numerical simulations of physical gels [7,12,27,28] is clearly evident. The plateaus indicate a timescale over which the acetone is sampling length scales larger than the liquid domain but smaller than the distance between liquid domains. The PGSE NMR data only contains signal from populations with  $T_2 \geq \tau_{\text{PGSE}}$ . This means acetone in a liquidlike domain during the first  $\tau_{\text{PGSE}}$  interval that samples the solidlike domain during the stimulated echo magnetization storage time, and then does not return to a liquidlike domain with  $T_2 \geq \tau_{\text{PGSE}}$  during the second  $\tau_{\text{PGSE}}$  interval, is not measured [46]. The data thus reflect the wait time distribution of solvent molecules trapped in low mobility solidlike regions and their transition to higher mobility regions [54]. The displacement time-dependent transition from the plateau to time-dependent  $\langle z^2(\Delta) \rangle$  is due to the diffusive length scale of acetone within the solidlike domain becoming greater than the distance between liquid domains. The plateaus occur at length scales of  $l_{\text{corr}} \sim [\langle z^2(\Delta) \rangle]^{1/2} = 710$  nm at 60 °C and 320 nm at 22 °C. The length scale from the diffusion data and the  $T_2$ - $T_2$  exchange data in the fast diffusion regime at 22 °C are in good agreement. The changes in the length scales observed correlate to changes in morphology above and below the glass transition temperature [46]. The MSD is subdiffusive  $\langle z^2(\Delta) \rangle \sim \Delta^\alpha$  after breaking out of the plateau caging region with  $\alpha = 0.69$  at 22 °C and 0.71 at 60 °C. Subdiffusive anomalous diffusion has been observed in microrheology studies using particles in polymer networks of PEO/water [55] and F-actin/water [56]. The observed subdiffusive dynamics of the solvent acetone at long displacement observation times indicate dynamic heterogeneity and are consistent

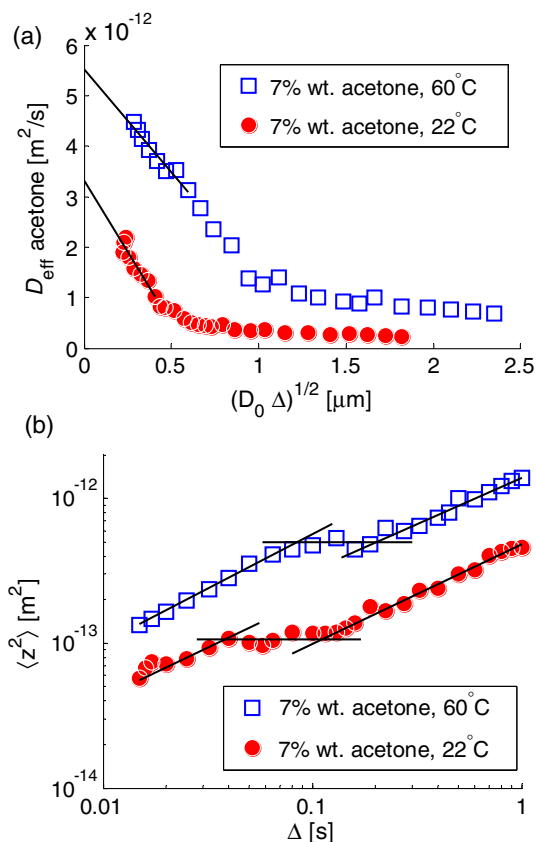


FIG. 4. PGSE measurements of (a) the effective acetone self-diffusion coefficient plotted against the diffusive length scale. The slope of the lines were used to find the ratio of pore volume to surface area. At 60°C,  $(V_p/S) = 1.4 \mu\text{m}$  and at 22°C,  $(V_p/S) = 590 \text{ nm}$ . (b) Mean squared displacement of acetone  $\langle z^2 \rangle$ . Lines are power law fits of the form  $\langle z^2(\Delta) \rangle \sim \Delta^\alpha$  to portions of the data. The MSD plateaus between 80–190 ms at 60°C and 40–130 ms at 22°C. The plateaus occur at a length scale of  $l_c \sim \langle z^2 \rangle^{1/2} = 710 \text{ nm}$  at 60°C and 320 nm at 22°C. The power law fits after the plateau region indicate subdiffusion with  $\alpha = 0.69$  (95% C.I. [0.63,0.75]) at 22°C and 0.71 (95% C.I. [0.61,0.81]) at 60°C.

with the continuous time random walk model proposed for glasses [54].

The 2D NMR relaxation data presented provide direct measurement of the existence of three domains of rotational mobility, dynamic heterogeneity, in a solvent-polymer HPMCAS/acetone system.  $T_1$ - $T_2$  correlation data show the change in solvent rotational mobility as a function of temperature and concentration, providing a direct means to monitor the glass transition in terms of solvent dynamics.  $T_2$ - $T_2$  exchange experiments and PGSE NMR measurements provide access to the solvent phase translational diffusion dynamics and provide quantitative length scale characterization. A mesoscale length  $\Xi = l_{\text{corr}}$  of the order of hundreds of nm is measured, in agreement with light scattering data of slow relaxation modes [30]. The length scale of spatial variation of the microscale cross-link

density related to network nanostructural heterogeneity [18]. The data demonstrate dynamic heterogeneity and glasslike dynamics in a physically associating solvent-polymer system at temperatures above and below the theoretical glass transition temperature indicating a weak gel-like structure above the glass transition temperature [9,16].

S. L. C. and J. D. S. acknowledge the late Paul T. Callaghan for providing the ILT software. The research was funded by Bend Research Inc. now Lonza Inc.

\*Corresponding author.

jseymour@montana.edu

- [1] T. Okuzono, K. y. Ozawa, and M. Doi, *Phys. Rev. Lett.* **97**, 136103 (2006).
- [2] D. T. Friesen, R. Shanker, M. Crew, D. T. Smithey, W. J. Curatolo, and J. A. S. Nightingale, *Mol. Pharmaceutics* **5**, 1003 (2008).
- [3] J. T. Moller and S. Fredsted, *Chem. Eng.* **116**, 34 (2009).
- [4] J. J. van Franeker, M. Turbiez, W. Li, M. M. Wienk, and R. A. J. Janssen, *Nat. Commun.* **6**, 6229 (2015).
- [5] J. S. Boateng, K. H. Matthews, H. N. E. Stevens, and G. M. Eccleston, *J. Pharm. Sci.* **97**, 2892 (2008).
- [6] J. D. Ferry, *Viscoelastic Properties of Polymers*, 3rd ed. (Wiley, New York, 1980).
- [7] S. K. Kumar and J. F. Douglas, *Phys. Rev. Lett.* **87**, 188301 (2001).
- [8] P.-G. de Gennes, *Scaling Concepts in Polymer Physics* (Cornell University Press, Ithaca, 1979).
- [9] S. B. Ross-Murphy, *J. Rheol.* **39**, 1451 (1995).
- [10] J. F. Douglas, *Gels* **4**, 19 (2018).
- [11] M. Rubinstein and R. H. Colby, *Polymer Physics* (Oxford University Press, Oxford, New York, 2003).
- [12] R. S. Hoy and G. H. Fredrickson, *J. Chem. Phys.* **131**, 224902 (2009).
- [13] H. H. Winter, *Macromolecules* **46**, 2425 (2013).
- [14] P. I. Hurtado, L. Berthier, and W. Kob, *Phys. Rev. Lett.* **98**, 135503 (2007).
- [15] P. J. Lu and D. A. Weitz, *Annu. Rev. Condens. Matter Phys.* **4**, 217 (2013).
- [16] S. R. Raghavan and J. F. Douglas, *Soft Matter* **8**, 8539 (2012).
- [17] M. H. Cohen and G. S. Grest, *Phys. Rev. B* **20**, 1077 (1979).
- [18] F. Di Lorenzo and S. Seiffert, *Polym. Chem.* **6**, 5515 (2015).
- [19] T. G. Fox and P. J. Flory, *J. Appl. Phys.* **21**, 581 (1950).
- [20] J. H. Gibbs and E. A. DiMarzio, *J. Chem. Phys.* **28**, 373 (1958).
- [21] Y. Q. Song, G. Carneiro, L. M. Schwartz, and D. L. Johnson, *Phys. Rev. Lett.* **113**, 235503 (2014).
- [22] P. T. Callaghan, *Translational Dynamics and Magnetic Resonance* (Oxford University Press Inc., New York, 2011).
- [23] P. P. Mitra, P. N. Sen, L. M. Schwartz, and P. Le Doussal, *Phys. Rev. Lett.* **68**, 3555 (1992).
- [24] K. E. Washburn and P. T. Callaghan, *Phys. Rev. Lett.* **97**, 175502 (2006).
- [25] T. G. Mason and D. A. Weitz, *Phys. Rev. Lett.* **74**, 1250 (1995).

- [26] T. M. Squires and T. G. Mason, *Annu. Rev. Fluid Mech.* **42**, 413 (2010).
- [27] E. Lascaris, M. Hemmati, S. V. Buldyrev, H. E. Stanley, and C. A. Angell, *J. Chem. Phys.* **142**, 104506 (2015).
- [28] E. R. Weeks and D. A. Weitz, *Phys. Rev. Lett.* **89**, 095704 (2002).
- [29] K. Kobayashi, C.-i. Huang, and T. P. Lodge, *Macromolecules* **32**, 7070 (1999).
- [30] J. Li, T. Ngai, and C. Wu, *Polym. J.* **42**, 609 (2010).
- [31] P. Sentosa, F. Fujara, and H. Sillescu, *Macromol. Chem. Phys.* **193**, 2421 (1992).
- [32] F. Fujara, B. Geil, H. Sillescu, and G. Fleischer, *Z. Phys. B* **88**, 195 (1992).
- [33] F. Mellinger, M. Wilhelm, and H. W. Spiess, *Macromolecules* **32**, 4686 (1999).
- [34] K. Schmidt-Rohr and H. W. Spiess, *Phys. Rev. Lett.* **66**, 3020 (1991).
- [35] J. Maquet, H. Théveneau, M. Djabourov, J. Leblond, and P. Papon, *Polymer* **27**, 1103 (1986).
- [36] R. A. Yapel, J. L. Duda, X. H. Lin, and E. D. Vonmeerwall, *Polymer* **35**, 2411 (1994).
- [37] M. E. Komlosh and P. T. Callaghan, *J. Chem. Phys.* **109**, 10053 (1998).
- [38] R. Kimmich and N. Fatkullin, *Polymer Chain Dynamics and NMR*, Advances in Polymer Science Vol. 170 (Springer, Berlin, Heidelberg, 2004).
- [39] P. T. Callaghan and A. Coy, *Phys. Rev. Lett.* **68**, 3176 (1992).
- [40] H. Walderhaug, O. Söderman, and D. Topgaard, *Prog. Nucl. Magn. Reson. Spectrosc.* **56**, 406 (2010).
- [41] F. Mallamace *et al.*, *J. Chem. Phys.* **127**, 045104 (2007).
- [42] Y. Q. Song, L. Venkataramanan, M. D. Hurlimann, M. Flaum, P. Frulla, and C. Straley, *J. Magn. Reson.* **154**, 261 (2002).
- [43] P. T. Callaghan, C. H. Arns, P. Galvosas, M. W. Hunter, Y. Qiao, and K. E. Washburn, *Magn. Reson. Imaging* **25**, 441 (2007).
- [44] AquaSolve ant AquaSolve AS hydroxypropylmethylcellulose acetate succinate physical and chemical properties handbook, (Ashland Inc.), [http://www.ashland.com/Ashland/Static/Documents/ASI/PC\\_12624\\_AquaSolve\\_AS\\_Handbook.pdf](http://www.ashland.com/Ashland/Static/Documents/ASI/PC_12624_AquaSolve_AS_Handbook.pdf) (accessed, 2014).
- [45] N. H. Williamson, A. M. Dower, S. L. Codd, A. L. Broadbent, S. R. Haug, R. Falk, J. Cape, D. T. Vodak, and J. D. Seymour, *Macromolecules* (to be published).
- [46] See, Supplemental Material at <http://link.aps.org/supplemental/10.1103/PhysRevLett.122.068001> for experimental details and additional data.
- [47] T. G. Fox, *Bull. Am. Phys. Soc.* **1**, 123 (1956).
- [48] C. A. Angell, J. M. Sare, and E. J. Sare, *J. Phys. Chem.* **82**, 2622 (1978).
- [49] B. Blümich, *NMR Imaging of Materials* (Clarendon Press, Oxford, 2000).
- [50] J. H. Lee, C. Labadie, C. S. Springer, and G. S. Harbison, *J. Am. Chem. Soc.* **115**, 7761 (1993).
- [51] L. Venturi, N. Woodward, D. Hibberd, N. Marigheto, A. Gravelle, G. Ferrante, and B. P. Hills, *Appl. Magn. Reson.* **33**, 213 (2008).
- [52] M. Van Landeghem, A. Haber, J.-B. D’Espinose De Lacaillerie, and B. Blümich, *Concepts Magn. Reson., Part A* **36A**, 153 (2010).
- [53] K. R. Brownstein and C. E. Tarr, *Phys. Rev. A* **19**, 2446 (1979).
- [54] J. S. Langer and S. Mukhopadhyay, *Phys. Rev. E* **77**, 061505 (2008).
- [55] J. Sprakel, J. van der Gucht, M. A. Cohen Stuart, and N. A. M. Besseling, *Phys. Rev. Lett.* **99**, 208301 (2007).
- [56] I. Y. Wong, M. L. Gardel, D. R. Reichman, E. R. Weeks, M. T. Valentine, A. R. Bausch, and D. A. Weitz, *Phys. Rev. Lett.* **92**, 178101 (2004).